Electrowetting on non-fluorinated hydrophobic surfaces

Han You
Andrew J. Steckl

Abstract — Fluorinated polymers, the most extensively used hydrophobic surface materials for electrowetting (EW) devices, are expensive and have potential risks to health and environment. In this paper, EW devices fabricated with non-fluorinated hydrophobic surfaces are demonstrated by using a polysiloxane-modified polyacrylate (BYK® Silclean® 3700, Louisville, KY). Water contact angle, which is the most critical parameter of EW devices, changes from ~165° to ~95° with a negligible hysteresis (~3°) when a 42 V AC voltage is applied. EW array display prototypes were constructed on the non-fluorinated surface and can be switched reversibly by applying a low voltage difference. These results indicate the promise of this BYK® Silclean® hydrophobic surface for EW devices in electronic readers and other mobile devices.

Keywords *— electrowetting, non-fluorinated.*

DOI # 10.1002/jsid.199

1 Introduction

When a voltage is applied between a sessile conducting droplet and a hydrophobic insulated surface, electrowetting (EW) occurs by modification of the electric charges present at the solid–liquid interface, resulting in contact angle (CA) change and wetting enhancement.[1,2] The EW effect offers a convenient method of fast and reversible control of the wetting properties of solid surfaces using electric fields. The interaction of light with an EW structure is controlled by the motion of two immiscible liquids (one clear and the other colored; one polar and the other non-polar), through their combined optical absorption, transmission, and reflection. Many important applications of the EW effect have recently been developed, such as adaptive lens systems,[3] lab-on-chip,[4] lipid bilayer membrane,[5] and microfluidic mixing and cleaning,[6,7] in addition to reflective displays.[8–11] Compared with other technologies, the EW reflective display screen has several advantages: it is very thin, operates at speeds suitable for video display,[12] has a wide viewing angle and relatively low power consumption.

The standard configuration of an EW structure consists of a sessile drop of a partially wetting conductive liquid (either in air or oil surrounding) on an electrically insulating dielectric layer covering a flat electrode, as shown in Fig. 1a. In addition to water, which has been the most extensively studied and commonly used EW fluid,[13,14] ionic liquids,[15,16] and non-aqueous organic fluids[17,18] have been used in the EW operation as the conductive liquids. The EW effect is a rather robust phenomenon that depends on the properties of the liquids and the dielectric layers, and on the interaction of these materials. Specifically, the properties of insulating layers are known to play an important role in lowering the driving voltage of EW devices.[19,20] To obtain a high initial CA of the conductive liquid, which results in larger CA change with voltage, the dielectric isolation typically consists of two layers: a hydrophobic layer on top of a thin insulating layer of high dielectric constant. Various materials have been investigated for the insulating layer: (a) inorganic insulators—SiO_2,[20] SiN,[21,22] Al_2O_3,[23,24] barium strontium titanate,[20] and bismuth zinc niobate[25]; (b) organic insulators, such as the parylene family—parylene N,[26] parylene C,[12,27] and parylene HT.[28]

The most commonly utilized hydrophobic materials in EW devices are amorphous fluoropolymers, such as Teflon AF,[20,26,29] Cytop,[8,30] and FluoroPel.[23,28] The strongly hydrophobic nature of the fluoropolymer enables the water droplet to sit on the surface with very high initial CA. However, such compounds carry relatively high cost and potential risks for human health and environment.[31] Hence, the use of a non-fluorinated hydrophobic insulating material is very important for the fabrication of environmentally friendly EW devices.

Presented herein are EW devices fabricated on non-fluorinated hydrophobic surfaces by using BYK® Silclean® 3700,[32] a commercially available polysiloxane-modified acrylate (PSXA) additive from BYK Additives & Instruments. This material is a widely used surface additive in coating and paints, and has been certified for food contact use. The OH-functional polysiloxane-modified polyacrylate (Fig. 1b) shows both good hydrophobic properties and reversible EW with both increasing and decreasing alternating current (AC) voltage. The water CA, which is the most critical parameter of EW devices, changes from ~165° to ~95° when a 42 V AC voltage is applied with a negligible hysteresis (~3°). EW arrays constructed on this non-fluorinated surface can be switched reversibly by applying a low voltage difference. These results indicate that BYK® Silclean® could be an ideal solution for

Received 07/2/13; accepted 12/10/13.
H. You and A. J. Steckl are with the Nanoelectronics Laboratory, Department of Electrical Engineering and Computing Systems, University of Cincinnati, Cincinnati, OH 45221-0030, USA; e-mail: a.steckl@uc.edu.

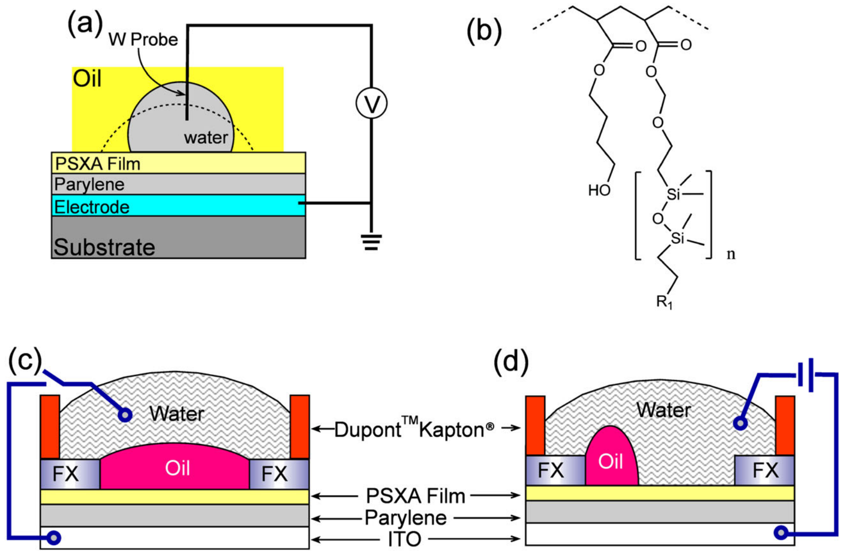

FIGURE 1 — Schematic diagrams illustrating the electrowetting operation with BYK PSXA (PSXA) as the hydrophobic layer: (a) EW test set up; (b) possible chemical structure of the BYK Silicone; (c) EW circular device without bias; (d) EW circular device with bias. FX is a hydrophilic negative photoresist (Dupont™ Riston® FX 915), which is patterned to provide the circular containment of the water droplet.

non-fluorinated hydrophobic surface in numerous low-voltage EW applications.

2 Experimental details

A schematic diagram of the EW structure and a circular EW device on a glass substrate is shown in Fig. 1. The basic EW structure is fabricated on a glass substrate and consists of a ground electrode, a dielectric layer, and the BYK® Silclean® top layer. Indium–tin oxide electrodes were sputtered in argon at 3.5 mTorr with 100 W direct-current (DC) power for 20 min. Next, a parylene layer was deposited using a LABCOATER® 2 parylene deposition unit (PDS 2010, Specialty Coating Systems, Indianapolis, IN) at room temperature. A 1 µm parylene layer was deposited using 0.8 g of starting material (parylene C, Specialty Coating Systems, Indianapolis, IN). The operating pressure was less than 15 mTorr. The parylene C surface is treated with oxygen plasma for ~ 1 min in order to provide the reaction site for the hydroxyl groups in the BYK PSXA material (Fig. 1b). The PSXA solution with a different concentration was then spin coated with 500 and 2500 rpm with 10 and 30 s, respectively, to obtain the hydrophobic layer. After UV exposure for 20 min, the film is heated at 80 °C for 30 min, in order to be cross-linked into the parylene C surface due to its OH-functionality, resulting in a hydrophobic film. Atomic force microscopy (AFM) (Veeco Dimension AFM, Plainview, WI) was used to characterize the surface morphology. The film thickness was measured by a profilometer and calibrated with an ellipsometer. EW tests were performed using water and a mixture of electrically insulating silicone oils (80 wt.% Dow Corning OS-20, 10 wt.% OS-10, and 10 wt.% OS-30, Germantown, NY). A clear acrylic box was used to contain the immersed substrate and fluids. A ~0.2 µL water droplet was injected onto the substrate and viewed through the

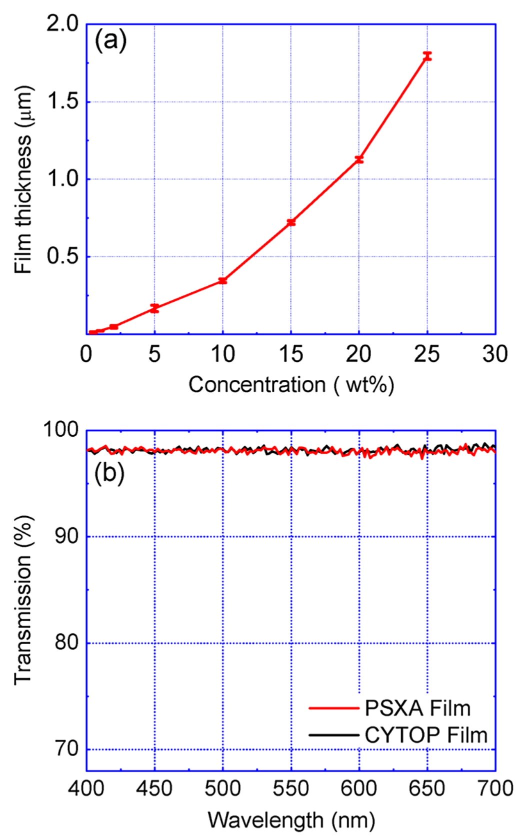

FIGURE 2 — BYK PSXA films: (a) thickness versus solution concentration of the solution; (b) optical transmission of BYK (PSXA) and conventional fluoropolymer (CYTOP) films versus wavelength for a 1 µm film.

transparent acrylic sidewalls. To provide electrical bias to the water droplet, a tungsten probe was inserted into the droplet. The other end of this probe was connected to the voltage supply, consisting of a power source (Tektronix AFG 3022BBeaverton, OR) amplified with a Trek 603 Lockport, NY). An FTA 1000B CA measurement system was used to record the CA data with the sessile drop method. The CA was obtained by averaging the right and left CA values. DC and AC (1 kHz, square wave) voltages up to 40 V with 2 V steps were applied. The CA measurement was taken after the voltage was applied for at least 3 s in order to reach equilibrium. For the DC voltage experiment, the bias is first ramped from 0 to +40 V with 2 V steps, until the droplet leaped off from the test spot. Then a new drop was injected to a new position to perform the negative bias experiment. The experiments were repeated at least three times at fresh sample locations and with fresh droplets for each test.

For the circular device, shown in Fig. 1b and 1c, the hydrophilic grid was formed using a negative photoresist (FX915 photoresist, DuPont™ Riston®, Durham, NC). FX915 film photoresist is hot-roll laminated to form a

TABLE 1 — Comparison between different hydrophobic materials

Hydrophobic materials	Teflon AF	CYTOP	FluoroPel	BYK PSXA
Structure	Amorp.	Amorp.	Amorp.	Amorp.
Phobic source	Fluor	Fluor	Fluor	Silicone
Optical trans. (1 μm)	>95%	>95%	>95%	>95%
Refractive index	1.31	1.34	1.35	1.49
Dielectric constant	1.93	2.0–2.1	2.25	4.52

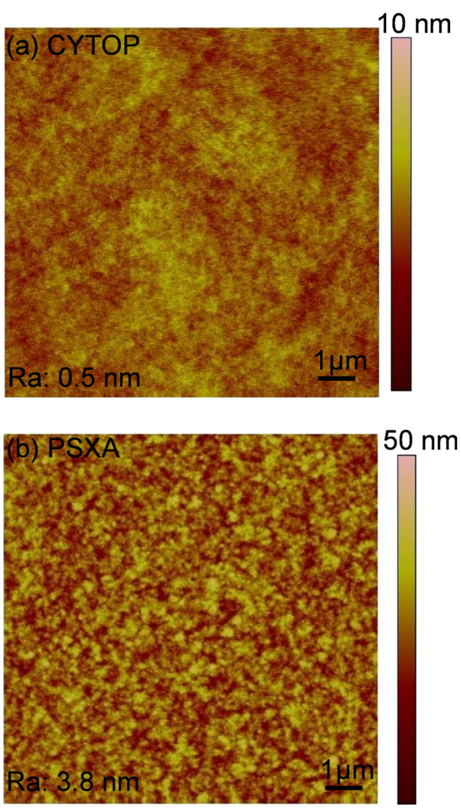

FIGURE 3 — AFM images and corresponding surface roughness (Ra) of the hydrophobic layer in the EW device: (a) CYTOP; (b) BYK PSXA (PSXA).

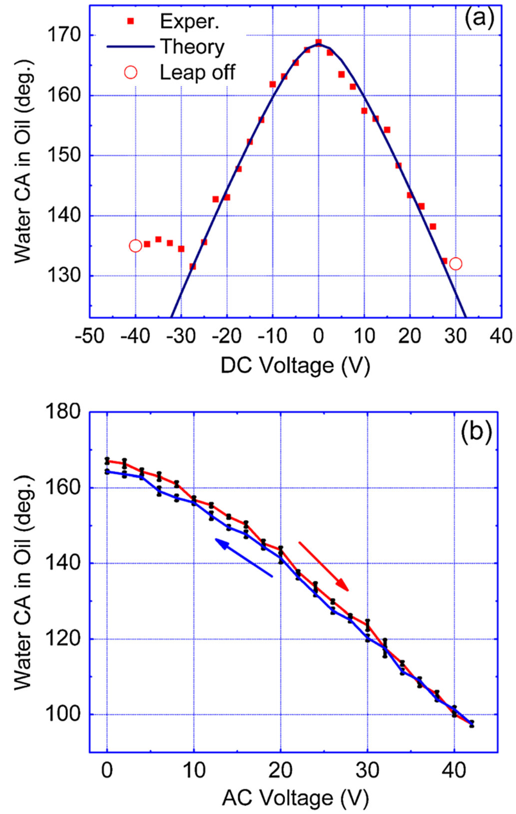

FIGURE 4 — Contact angle of 0.2 μL water droplet in silicone oil on BYK PSXA film as a function of applied bias: (a) comparison between experimental (points) and calculated (line) CA versus DC voltage ; (b) 1 kHz AC voltage (RMS).

~15 μm film and then photolithographically patterned. A hydrophobic grid, made of polyimide-based tape (Dupont™ Kapton®, Torrance, CA), was used to contain the water volume. To operate the EW device, typically a ~80 μL droplet of deionized (DI) water was first placed on the hydrophobic surface. Then, ~40 nL of dodecane (Acros, Pittsburgh, PA) with a nonpolar red dye (Keystone Aniline Corp., Chicago, IL, 3 wt.%) was injected using a nano-injector system (Stoelting Co., Wood Dale, IL). The active device area is defined by the hydrophilic grid, which confines the oil by strongly attracting the water. The oil injection process was monitored by a color CCD camera system (Diagnostic Instrument, Sterling Heights, MI) for top view and CCD color video camera system (Sony, San Jose, CA) with TV zoom lens (Navitron, Benton Harbor, MI) for side view. When a bias is applied to the water droplet, the resulting field across the hydrophobic insulator effectively increases its surface energy and reduces its hydrophobicity, attracting the polar water molecules to the insulator surface. The water increasingly displaces the oil layer to the side region of the structure with increasing bias.

3 Results and discussion

For the initial set of experiments, BYK PSXA films formed from solutions with different concentrations were evaluated.

The as-received BYK® Silclean® solution is 25 wt.% silicone-modified polyacrylate in methoxypropylacetate, which produces 1.8 µm film by spin coating. However, using such a thick BYK film as the only layer for dielectric and hydrophobic function results in rather poor EW properties. Thinner films can be obtained by decreasing concentration, as shown in Fig. 2a. If the solution is diluted to 1 wt.%, the film thickness decreases to ~22 nm, which is close to the typical thickness of the fluoropolymer layer used in EW device.[12] This thickness is therefore chosen for the investigation of EW effect. Figure 2b shows the optical transmission over the visible spectrum of 1 µm film of BYK PSXA and reference fluoropolymer (CYTOP), respectively. It can be seen that the BYK PSXA film is fully transparent in the visible range with nearly 100% transmission, which is very important if EW device is used in the transmissive mode. Selected properties of the BYK PSXA film and conventional fluoropolymers are shown in Table 1. The BYK PSXA film has a relatively high dielectric constant (~4.5) and refractive index (1.5). The higher dielectric constant makes it potentially a better dielectric layer in EW devices.

The film surface morphology also influences the EW characteristics of structures. Figure 3b contains an AFM image of the BYK film surface. For comparison, the AFM scan of the surface of CYTOP film (40 nm) is shown in Fig. 3a, as CYTOP is a common fluoropolymer used in EW devices. The insets in Fig. 3a and 3b shows the root mean square (RMS) values of the corresponding surfaces. While the CYTOP surface has an excellent surface with a roughness of only ~0.5 nm, the BYK PSXA film (22 nm) does exhibit a reasonably smooth surface morphology with an RMS roughness value of 3.8 nm.

The EW effect on the BYK PSXA film (22 nm) was evaluated by measuring the CA of water droplets immersed in a mixture silicone oils (OS-20 : OS-10 : OS-30 = 8:1:1; $\gamma = 16.1$ mN/m) as a function of applied voltage. Over a considerable voltage range, the experimental CA data are in agreement with values calculated from EW theory.[12] As shown in Fig. 4a, the initial CA of a 0.2 µL DI water droplet in oil on the BYK PSXA surface is ~168°, decreasing to ~132° as the DC voltage increase to ±28 V. Lower angles may be possible, but the droplet tends to leap from the probe electrode, probably because of inhomogeneous charge injection.[33] For AC bias experiments, a 1 kHz square-wave signal was applied to the water droplet. As shown in Fig. 4b, a ΔCA of 70° is obtained between zero bias and 42 V rms, which is almost the same as that obtained from EW devices with conventional fluoropolymer hydrophobic surfaces.[11] The maximum AC voltage used in this EW device is 42 V rms

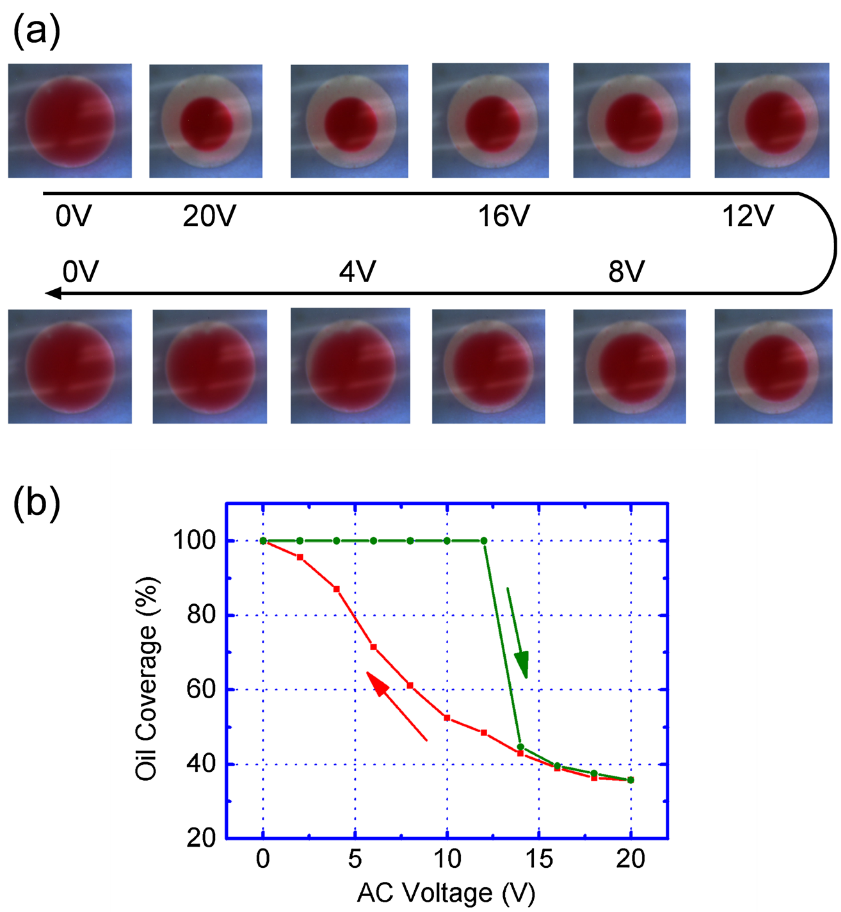

FIGURE 5 — Oil (60 nL of dodecane) coverage as a function of 1 kHz AC voltage (RMS) in a circular EW device (1.4 mm diameter): (a) photographs of the device at different voltages; (b) oil coverage area versus RMS voltage in increasing (green) and decreasing (red) directions.

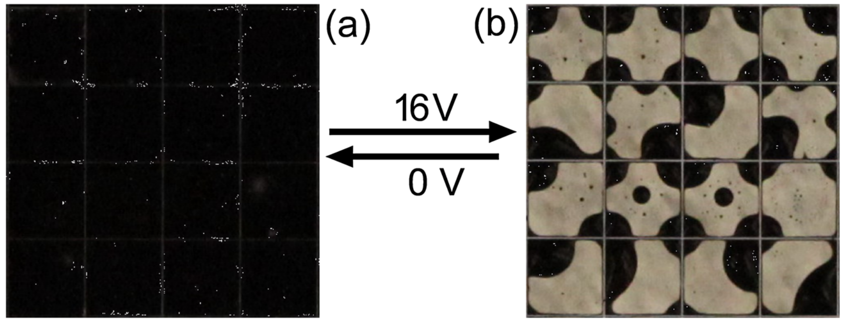

FIGURE 6 — EW switching of a 4 × 4 pixel array on the BYK® Silclean® surface with $1.5 \times 1.5\,mm^2$ pixels: (a) zero bias; (b) 16 V (RMS), 1 kHz.

in order to prevent dielectric breakdown, which occurs at ~50 V for these devices.[34] Reversing the direction of voltage sweep, the CA of the water droplet recovers to ~163°, which is very close to the initial CA. Most important, a very low hysteresis was observed (with a maximum value of 3°). This characteristic is very useful for actual EW applications.

Circular EW devices are fabricated on glass substrates to evaluate the EW pixel operation through oil coverage change with the applied voltage. The results are illustrated in Figs. 5a. The two fluids in the device are the polar conducting (DI water) component and the insulating non-polar (colored dodecane) component. Fluid motion in the device is governed by the EW effect. Oil coverage as a function of AC voltage is illustrated in Fig. 5a, taken at different applied voltages (1 kHz waveform). EW device at zero bias has 100% oil coverage, which is defined by the surface tension. EW starts at 14 V rms, as shown in Fig. 5b, which is required to initiate the movement of the colored oil film.[35] The oil-covered area decreases to 35% of the total area as the bias is gradually increased to 20 V rms, as shown in Fig. 5b. At higher voltages (~40 V), the oil will displace to the side walls of the pixel, and oil coverage as low as 10% of the device area can be reached. However, the high voltage will reduce the repeatability of EW operation. When the bias is then decreased back to 0 V, the displaced oil returns and covers the entire device area again (100% coverage). The process can be repeated for many cycles (>10) as the AC voltage is changed.

Arrays of EW pixels of 1.5 mm × 1.5 mm (20 × 20 array) were fabricated using the BYK PSXA film as the hydrophobic layer. The structure of the array pixel is the same as that of the circular pixel. Each pixel contained a black dye mixed in tetradecane oil. In the OFF state, the black oil occupied the entire pixel area because of the surface tension, as shown in Fig. 6a. When a voltage was applied, the EW force displaced the black oil into the corner of each pixel, resulting in a mostly clear pixel, as shown in Fig. 6b, for a voltage of 16 V rms (1 kHz). After the voltage was withdrawn, the oil once again covered the entire pixel. Adjusting the voltage controls the oil coverage (and resulting transmission) in the pixel, which determines the gray scale of the EW array.

4 Summary and conclusions

In this study, we successfully demonstrated that non-fluorinated material BYK® Silclean® produces hydrophobic film suitable for EW applications. The EW devices with the BYK PSXA film showed large CA modulation (~70°) and very low hysteresis (~3°), which is sufficient for many EW applications. EW array display prototypes with the BYK PSXA hydrophobic surface were fabricated and were shown to be switched reversibly by applying a low voltage difference. These results indicate that BYK® Silclean® could be an ideal solution for non-fluorinated hydrophobic surface in different EW applications.

Acknowledgments

The authors want to thank John Du from BYK Additives and Instruments for generously providing the Silclean® 3700 and Andy Sebastian of RJ Reynolds for many useful discussions and support of this research.

References

1 F. Mugele and J. C. Baret, “Electrowetting: from basics to applications,” *J. Phys. Condens. Matter* **17**, No. 28, R705 (2005).

2 F. Mugele, “Fundamental challenges in electrowetting: from equilibrium shapes to contact angle saturation and drop dynamics,” *Soft Matter* **5**, No. **18**, 3377–3384 (2009).

3 M. Vallet *et al*., “Limiting phenomena for the spreading of water on polymer films by electrowetting,” *Eur. Phys. J. B* **11**, No. 4, 583–591 (1999).

4 A. Banerjee *et al*., “Reconfigurable virtual electrowetting channels,” *Lab Chip* **12**, No. 4, 758–764 (2012).

5 S. Punnamaraju and A. J. Steckl, “Voltage control of droplet interface bilayer lipid membrane dimensions,” *Langmuir* **27**, No. 2, 618–626 (2011).

6 F. Mugele *et al*., “Capillary Stokes drift: a new driving mechanism for mixing in AC-electrowetting,” *Lab Chip* **11**, No. 12, 2011–2016 (2011).

7 M. Jonsson-Niedziolka *et al*., "EWOD driven cleaning of bioparticles on hydrophobic and superhydrophobic surfaces," *Lab Chip* **11**, No. 3, 490–496 (2011).

8 H. You and A. J. Steckl, “Three-color electrowetting display device for electronic paper,” *Appl. Phys. Lett.* **97**, No. 2, 023514 (2010).

9 J. Heikenfeld *et al*., “Electrofluidic displays using Young–Laplace transposition of brilliant pigment dispersions,” *Nat. Photonics* **3**, No. 5, 292 (2009).

10 R. A. Hayes and B. J. Feenstra, "Video-speed electronic paper based on electrowetting," *Nature* **425**, No. 6956, 383 (2003).
11 D. Y. Kim and A. J. Steckl, "Electrowetting on paper for electronic paper display," *ACS Appl. Mater. Interfaces* **2**, No. 11, 3318–3323 (2011).
12 H. You and A. J. Steckl, "Electrowetting on flexible substrates," *J. Adhesion Sci. Technol.* **26**, No. 12–17, 1931–1939 (2012).
13 J. Heikenfeld and A. J. Steckl, "High-transmission electrowetting light valves," *Appl. Phys. Lett.* **86**, No. 15, 151121 (2005).
14 B. Raj *et al*., "Ion and liquid dependent dielectric failure in electrowetting systems," *Langmuir* **25**, No. 20, 12387–12392 (2009).
15 S. Millefiorini *et al*., "Electrowetting of ionic liquids," *J. Am. Chem. Soc.* **128**, No. 9, 3098–3101 (2006).
16 Y. S. Nanayakkara *et al*., "A fundamental study on electrowetting by traditional and multifunctional ionic liquids: possible use in electrowetting on dielectric-based microfluidic applications," *Anal. Chem.* **80**, No. 20, 7690–7698 (2008).
17 S. Chevalliot *et al*., "Analysis of nonaqueous electrowetting fluids for displays," *J. Display Technol.* **7**, No. 12, 649–656 (2011).
18 D. Chatterjee *et al*., "Droplet-based microfluidics with nonaqueous solvents and solutions," *Lab Chip* **6**, No. 2, 199–206 (2006).
19 X. Zhang and Y. Cai, "Ultralow voltage electrowetting on a solidlike ionic-liquid dielectric layer," *Angew. Chem. Int. Ed. Engl.* **52**, No. 8, 2289–2292 (2013).
20 H. Moon *et al*., "Low voltage electrowetting-on-dielectric," *J. Appl. Phys.* **92**, No. 7, 4080–4087 (2002).
21 T. Krupenkin *et al*., "Tunable liquid microlens," *Appl. Phys. Lett.* **82**, No. 3, 316–318 (2003).
22 B. R. Acharya *et al*., "Tunable optical fiber devices based on broadband long-period gratings and pumped microfluidics," *Appl. Phys. Lett.* **83**, No. 24, 4912–4914 (2003).
23 D. Y. Kim and A. J. Steckl, "Complementary electrowetting devices on plasma treated fluoropolymer surfaces," *Langmuir* **26**, No. 12, 9474–9483 (2010).
24 J. Zhang *et al*., "Preparation and analysis of 1-chloronaphthalene for highly refractive electrowetting optics," *Langmuir* **25**, No. 17, 10413–10416 (2009).
25 N. Y. Kim *et al*., "The movement of micro droplet with the effects of dielectric layer and hydrophobic surface treatment with R.F. atmospheric plasma in EWOD structure," *J. Phys.: Conf. Series* **34**, No. 1, 650 (2006).
26 M. W. J. Prins *et al*., "Fluid control in multichannel structures by electrocapillary pressure," *Science* **291**, No. 5502, 277–280 (2001).
27 W. J. J. Welters and L. G. J. Fokkink, "Fast electrically switchable capillary effects," *Langmuir* **14**, No. 7, 1535–1538 (1998).
28 M. Dhindsa *et al*., "Reliable and low-voltage electrowetting on thin parylene films," *Thin Solid Films* **519**, No. 10, 3346–3351.
29 E. Seyrat and R. A. Hayes, "Amorphous fluoropolymers as insulators for reversible low-voltage electrowetting," *J. Appl. Phys.* **90**, No. 3, 1383–1386 (2001).
30 S. Berry *et al*., "Irreversible electrowetting on thin fluoropolymer films," *Langmuir* **23**, No. 24, 12429–12435 (2007).
31 M. M. Schultz *et al*., "Fluorinated alkyl surfactants," *Environ. Eng. Sci.* **20**, No. 5, 487–501 (2003).
32 C. Nagel *et al*., "New silicone structures," *Eur. Coat. J.* **04**, No. 1, 32–39 (2010).
33 A. I. Drygiannakis *et al*., "On the connection between dielectric breakdown strength, trapping of charge, and contact angle saturation in electrowetting," *Langmuir* **25**, No. 1, 147–152 (2008).
34 A. Schultz *et al*., "Detailed analysis of defect reduction in electrowetting dielectrics through a two-layer 'barrier' approach," *Thin Solid Films* **534**, 348–355 (2013).
35 T. Roques-Carmes *et al*., "A physical model describing the electro-optic behavior of switchable optical elements based on electrowetting," *J. Appl. Phys.* **96**, No. 11, 6267–6271 (2004).

Han You received his PhD degree in Polymer Chemistry and Physics from Changchun Institution of Applied Chemistry, Chinese Academy of Science (China). After receiving his PhD, he moved to the Nanoelectronics Lab at the University of Cincinnati as a post-doctoral researcher fellow. His research interest is focused on organic electronic devices and electrowetting devices.

Dr. Andrew J. Steckl is Ohio Eminent Scholar and Carl Gieringer Professor of Solid State Electronics at the University of Cincinnati, where he directs the Nanoelectronics Laboratory. He has been a faculty member at Cincinnati since 1988. Previously, he was on the faculty at Rensselaer Polytechnic Institute, where he founded the Center for Integrated Electronics. Dr. Steckl obtained his BS from Princeton and his PhD from the University of Rochester. Dr. Steckl is a Fellow of IEEE and AAAS. At Cincinnati, he received numerous awards, including the Rieveschl Award for Distinguished Scientific Research, Distinguished Engineering Research Award, and Graduate Faculty Fellow. In 2013, he was named Distinguished Research Professor. Dr. Steckl's current research areas of interest include (organic and inorganic) light-emitting materials and devices and electrofluidics (electrowetting and electrospinning). Together with his students, he has published over 400 articles and obtained 16 patents, with a current citation *h*-index of 50.